NARROW BAND GAP SEMICONDUCTORS

Narrow band gap semiconductors are defined as semiconductors with an energy band gap smaller than that of silicon. Figure 1 shows the energy band gap versus the lattice constant plot for major semiconductors. The area of the narrow band gap semiconductors is marked with the slant lines. Several important narrow band gap semiconductors are displayed in the figure. One is the elementary semiconductor Ge with the lattice in the diamond structure. Other key ones are III-V and II-VI compound semiconductors: InAs, GaSb, InSb, and HgCdTe, whose lattice is in the zincblende structure. Also shown in the figure are three lead salts, PbS, PbSe, and PbTe, whose lattice is in the rock-salt (NaCl) structure. The structures of all these narrow band gap semiconductors are composed of two interpenetrating face centered cubic (fcc) lattices (1) with the lattice constant a_0 defined as the length of the fcc cube edge. For the diamond and the zincblende structures, each fcc lattice is shifted by $a_0/4$ (111) to the other lattice, whereas in the rock-salt structure, the shifting vector is $a_0/2$ (100). After describing the fundamental structures, the properties and the related devices of each narrow band gap semiconductor are described briefly as follows.

Ge was an important semiconductor material used for electronics before the emerging of the modern Si technology. It has an indirect band gap energy of 0.664 eV (2) at room temperature as observed in Fig. 1. Interestingly, its lattice constant is close to that of GaAs, which has been taken advantage of to allow the deposition of high-quality GaAs-based materials on Ge for use in implementing the InGaP/InGaAs/Ge triple-junction tandem solar cell (3), which has a record conversion efficiency of about 40%. Another important application of Ge is infrared detectors. Despite the large lattice mismatch between Si and Ge as observed in Fig. 1, the alloy SiGe has been successfully used to realize the Si heterojunction bipolar transistor (HBT) (4). Because of a smaller band gap as compared with Si, SiGe has been used to implement the base of the Si HBT with a very narrow base width, SiGe-base HBT, which allows a heavy p-type doping density without deteriorating the electron injection efficiency. Because of the very small base width and the very low base resistance, SiGe-base HBT has become an important high-speed semiconductor device for use in Si integrated circuits needed for wireless communications.

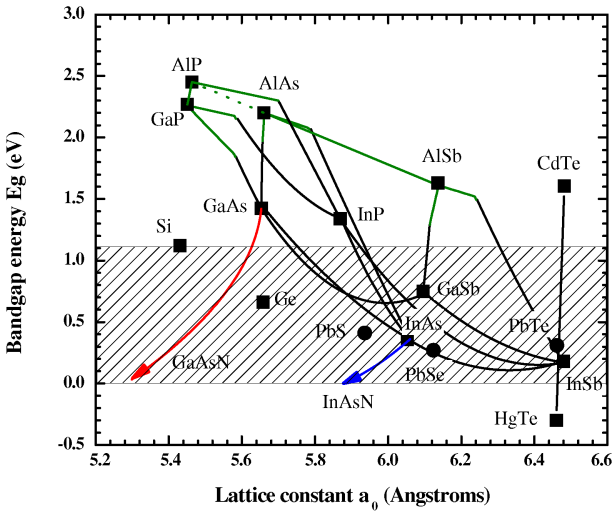

Figure 1. Energy band gap versus lattice constant plot for major semiconductors. The area for narrow band gap semiconductors is marked with slant lines.

InAs has an energy band gap of 0.354 eV at room temperature (2). In the 1960s, the light-emitting diode and the laser diode were realized based on InAs (5). For the past decades, its alloy InGaAs has been intensely studied to be used for implementing electronic and photonic devices. Because it is lattice-matched with InP, InGaAs is a basic material for realizing devices used in optical fiber communication (6) and high-speed electronics (7). Thanks to the superior transport properties resulting from a small electron effective mass, the InGaAs-base HBT and the InGaAs-channel high electron mobility transistor (HEMT) have been created for implementing high-speed communication integrated circuits such as the 40-Gb transimpedance amplifier (8). Because GaAs is a more mature material as compared with InP, the structure of InGaAs on GaAs has raised a substantial amount of attention for industrial and academic research. As the lattice constant of InGaAs is larger than that of GaAs, the strained InGaAs/GaAs quantum well (QW) and the metamorphic InGaAs (9) structures on the GaAs substrate have been successfully developed. The strained InGaAs/GaAs QW structure on the GaAs substrate is used to implement pseudomorphic HEMTs and lasers. The metamorphic InGaAs structure on the GaAs substrate is used for realizing HEMTs. Because of the constraints on the thickness and the In composition (10), the lowest inter-band transition energy of the strained InGaAs QW structure on the GaAs substrate is about 1 eV (11). The transition energy could be lowered by the diluted nitride InGaAsN solutions. The band gap energy and the lattice constant could be simultaneously reduced by incorporating a tiny amount of nitrogen (less than 3%) in the traditional III–V compound semiconductors. As shown in Fig. 1, the boundary of the quaternary InGaAsN material is GaAsN and InAsN as indicated in blue and red curves. The energy band gap reduction using the diluted nitrides could be explained using the band-anticrossing model (12). Incorporation of the highly electronegative nitrogen atoms gives rise to the localized energy levels close to the conduction band edge of the host semiconductor. The hybridization between the localize states and the conduction band results in two modified bands. The lower band, caused by the repulsive effect, is lower than the original band of the host semiconductor. As a result, the strained InGaAsN/GaAs QW structure could have a transition wavelength as long as 1520 nm (13), which has been used to realize the 1300-nm vertical cavity surface emitting lasers (VCSELs) for optical communication (14). Because of the lattice contraction resulting from the nitrogen incorporation, $In_xGa_{1-x}As_{1-y}N_y$, with $x \sim 3y$, can be lattice-matched with GaAs, thus becoming a promising material for the tandem solar cells (15). Currently, most high-efficiency tandem solar cells are composed of three sub-cells: InGaP, InGaAs, and Ge. For a further higher efficiency, the targeted energy band gap of the

fourth cell is about 1 eV, where InGaAsN is a promising candidate.

Another important structure on the GaAs substrate for long transition wavelength applications is the InAs self-assembled quantum dot (QD) (16). The formation of the InAs QD is from the about 7% lattice mismatch between GaAs and InAs. The accumulating strain energy during the deposition of InAs turns the growth mode from the layer-by-layer mode to the island mode as the nominal deposition thickness reaches 1.7 monolayers (17). From a photoluminescence (PL) study, the PL wavelength of the bared InAs QD on GaAs can be as long as 1500 nm. However, the compression and the In/Ga atomic interchange resulting from the overgrown GaAs capping layer needed for realizing devices shift the transition energy up to about 1 eV. By inserting a thin InGaAs layer between the InAs QD and the GaAs capping layer, the compression and the atomic exchange could be reduced, leading to the extension of transition wavelength to over 1300 nm (18, 19). Insertion layers using other materials such as AlGaAs, GaAsSb, and InGaAsN have also been studied to manipulate the composition and the shape of the QD to obtain a longer emission wavelength (20, 21). As a result, 1300-nm VCSEL with the InAs QD active medium has been realized on the GaAs substrate (22).

GaSb has an energy band gap of 0.725 eV at 300 K (23). GaSb is particularly important as a substrate material for the Sb-based alloys, whose energy band gap is in the mid-infrared wavelength range. It is interesting that the spin-orbit splitting of the valence band is almost equal to the energy band gap of GaSb, which results in a high hole ionization coefficient. Therefore, a significant advantage in the signal-to-noise ratio property has been obtained from the GaSb-based avalanche photodetectors. The mixed alloy of GaAs and GaSb is a promising material for optoelectronic and electronic device applications. GaAsSb, which is lattice-matched with InP, has been used as the base of the InP/GaAsSb NPN double HBT (24, 25). Because the band lineup between InP and GaAsSb is type-II, this HBT is free from the complicated base-collector junction grading, which is used to avoid the annoying current blocking and the reach-through effects commonly observed in the HBT with the type-I base-collector band discontinuity (26). As the As mole fraction is larger than 0.6, GaAsSb has its lattice constant and energy gap relation close to that of InGaAs with the same As mole fraction. According to several reports (27, 28), the band lineup of the GaAsSb/GaAs QW structure is composition dependent. The alignment is weak type-I for a small Sb mole fraction and turns out to be type-II as the fraction increases. These types of band lineup make the electrons stay in GaAs and the holes in GaAsSb. Although the spatial separation lowers the dipole matrix element of the electron hole recombination, their transition energy can be lower than the fundamental energy gap of either GaAsSb or GaAs, which is beneficial for long wavelength applications. Overall, 1300-nm lasers of edge- or vertical-emitting type on the GaAs substrate (29, 30) have been developed. The diluted-nitride GaAsSbN material has also been intensely studied (31). This quaternary alloy has a better thermal stability than InGaAsN because it has only one group III element, thus free from the InN/GaN bond change during the heat treatment (32). As post-growth annealing is necessary for the diluted nitrides to result in a good device quality, this behavior could be taken advantage of to result in a smaller blue shift in wavelength due to the chemical change for the GaAsSbN material. The p-i-n detector with a cutoff wavelength longer than 1300 nm using GaAsSbN, which is lattice-matched with GaAs, with an energy gap below 1 eV has been reported (33). In addition, the strained quinternary InGaAsSbN QW structure has also been used in lasers operating at 1600 nm on the GaAs substrate (34, 35).

Sb-based alloys grown on the InAs or GaSb substrate are important semiconductors for mid-infrared optoelectronic devices. Several chemical gases and liquids have a strong signature absorption in the mid-infrared wavelength range. The development of the Sb-based semiconductors can provide miniature and low-cost emitters and detectors for device engineering in this wavelength band. The InAsSb alloy is an important material for this application because it has the lowest energy gap (0.108 eV for an Sb fraction of 0.65 (36)) in III–V compounds at room temperature. Experimental and theoretical studies pointed out that the As-rich InAsSb/InAs structure is a staggered type-II heterojunction when the InAsSb is strained (37). Lasers based on this type of the InAsSb/InAs heterojunction have been demonstrated at cryogenic temperature (38). However, high-temperature operation is limited by Auger recombination and inter-valence band absorption (39). Type-I InGaAsSb/AlGaAsSb heterojunction has been also successfully applied as an active medium for lasers operating at room temperature (40). However, its threshold current increases rapidly as the wavelength is longer than 3 μm, which is attributed to hole leakage and Auger recombination. Much more sophisticated devices called inter-band cascade lasers with the "W-shape" QW structure have been designed to extend the wavelength of the laser operating at room temperature (41). The structure uses the type-II broken gap QW in four layers, for example InAs/InGaSb/InAs/AlGaAsSb, in each period with the "W-shape" conduction band profile. The type-II lineup of InAs/InGaSb allows the tailoring of the electronic states for Auger recombination suppression (42), whereas the "W-shape" conduction profile can concentrate the electron wave function and improve the radiative recombination. Furthermore, a carefully designed broken gap heterostructure between the laser stages also allows the recombined electrons in the valence band to tunnel to the conduction band of the next stage for another radiative recombination (43). Strip inter-band cascade lasers have reached the 3.38-μm CW operation at 350 K (41).

Alloy $Hg_{1-x}Cd_xTe$ is an important narrow gap semiconductor for infrared detectors and image sensors (44). HgTe and CdTe, the alloy made of the binaries, are II–VI compounds in the zincblende lattice structure. The energy gap of CdTe is 1.606 eV, larger than Si. On the other hand, HgTe is a semi-metal, having its Γ_6 band state—the conduction band bottom, lower than its Γ_8 band state—the valence band top, by 0.3 eV. The energy gap of the alloy

$Hg_{1-x}Cd_xTe$ can be expressed as

$$E_g(T) = 1.59x - 0.25 + 5.233 \times 10^{-4}\,T\,(1 - 2.08\,x) + 0.327\,x^3\ \text{eV}.$$

The temperature coefficient of HgTe is positive, which is opposite to those of CdTe and other ordinary semiconductors. Therefore, the coefficient of the alloy is composition dependent. The lattice constants of CdTe and HgTe are 6.482 Å and 6.46 Å, respectively. The alloy is usually grown on the CdTe substrate because of excellent lattice match and chemical compatibility. In the 1970s, HgCdTe photoconductive detector technology progressed rapidly. The wavelength of the detectors developed covers 1–3, 3–5, 8–12, and 15–30 μm (44). Detector linear arrays of 60–180 elements have been in mass production for military and civilian applications (45).

Lead salts include PbS, PbSe, and PbTe. They are IV–VI compound semiconductors with the crystalline in the rock-salt structure (NaCl). These semiconductors have the L direct band; i.e., the top of the valence band and the bottom of the conduction band occur in the (111) direction at $k = \pi/a$ (46). The energy gaps at room temperature for PbS, PbSe, and PbTe are 0.41, 0.27, and 0.31 eV, respectively (47). The temperature coefficients of these energy gaps are positive, which is opposite to those for Si and III–V compounds. Lead salt laser is the oldest mid-infrared emitter, and for many years, they are the only commercially available mid-infrared sources. $Pb_{1-x}Sn_xTe$, which is a mixed alloy of PbTe and SnTe, an IV–VI compound with the energy gap strongly depending on the carrier concentration, has an energy gap of $E_g(eV) = 0.19 - 0.543x$ at 12 K (48). The energy gap vanishes as x approaches 0.35. The most successful IV–VI lasers are based on the PbTe/PbSnTe heterostructure. Another alloy $PbS_{1-x}Se_x$ has an energy gap of $E_g(eV) = 0.289 - 0.144x$ at 12 K (49). Lasers based on PhS/PbSSe have been also successfully created. The electrically pumping lead salt lasers have achieved the 333 K operation in pulsed mode (50). The above room temperature operation is caused largely by the low Auger recombination rate in the IV–VI system. The Auger coefficients of the lead salts are generally an order of magnitude smaller than those in III–V compounds with the same energy gap. However, as compared with III–V materials, the lead salts, which are more susceptible to damage, have lower thermal conductivities. Thus, their output power is limited to below 1 mW (51).

BIBLIOGRAPHY

1. C. Kittel, *Introduction to Solid State Physics*, Chapter 1, 8th ed., John Wiley and Sons, Inc., New York, 2005.
2. O. Madelung, *Semiconductors—Basic Data*, 2nd revised ed., Springer, Germany, 1996.
3. M. Yamaguchi, T. Takamoto, and K. Araki, "Super high-efficiency multi-junction and concentrator solar cells," *Solar Energy Materials & Solar Cells* **90**, 3068–3077, 2006.
4. A. J. Joseph, D. L. Harame, B. Jagannathan, D. Coolbaugh, D. Ahlgren, J. Magerlein, L. Lanzerotti, N. Feilchenfeld, S. St Onge, J. Dunn, and E. Nowak, "Status and direction of communication technologies—SiGe BiCMOS and RFCMOS," *Proceedings of the IEEE* **93**, 1539–1558, 2005.
5. I. Melngailis and R. H. Rediker, "Properties of InAs lasers," *J. Appl. Phys.* **37**, 899–911, 1966.
6. G. P. Agrawal and N. K. Dutta, *Long-Wavelength Semiconductor Lasers*, Van Nostrand Reinhold, USA, 1986.
7. O. Wada, and H. Hasegawa, *InP-Based Materials and Devices*, John Wiley and Sons, Inc. New York, 1999.
8. M. Sokolich, "High speed, low power, optoelectronic InP-based HBT Integrated circuits," *IEEE 2002 Custom Integrated Circuits Conference*, 483–490, 2002.
9. P. M. Smith, D. Dugas, K. Chu, K. Nichols, K. G. Duh, J. Fisher, L. Mt Pleasant, D. Xu, L. Gunter, A. Vera, R. Lender, and D. Meharry, "Progress in GaAs metamorphic HEMT technology for microwave applications," *Annual Technical Digest of 25th IEEE Gallium Arsenide Integrated Circuit (GaAs IC) Symposium*, 21–24, 2003.
10. J. W. Matthews and A. E. Blakeslee, "Defects in epitaxial multilayers," *J. Crystal Growth* **27**, 118–125, 1974.
11. L. W. Sung and H. H. Lin, "Highly-strained 1.24-μm InGaAs/GaAs quantum-well lasers," *Appl. Phys. Lett.* **83**, 1107–1109, 2003.
12. W. Shan, W. Walukiewicz, J. W. Ager III, E. E. Haller, J. F. Geisz, D. J. Friedman, J. M. Olson, and S. R. Kurtz, "Band anticrossing in GaInNAs alloys," *Phys. Rev. Lett.* **82**, 1221–1224, 1999.
13. M. Fischer, M. Reinhardt, and A. Forchel, "GalnAsN/GaAs laser diodes operating at 1.52μm," *Electron. Lett.* **36–37**, 1208, 2000.
14. J. S. Harris, "Tunable long-wavelength vertical-cavity lasers: the engine of next generation optical networks," *IEEE J. Select. Topics Quantum Electron.* **6**, 1145–1160, 2000.
15. D. J. Friedman, J. F. Geisz, S. R. Kurtz, and J. M. Olson, "1-eV solar cells with GaInNAs active layer," *J. Crystal Growth* **195**, 409–414, 1998.
16. N. N. Ledentsov, M. Grundmann, F. Heinrichsdorff, Dieter Bimberg, V. M. Ustinov, A. E. Zhukov, M. V. Maximov, Zh. I. Alferov, and J. A. Lott, "Quantum-dot heterostructure lasers," *IEEE J. Select. Topics Quantum Electron.* **6**, 439–451, 2000.
17. P. B. Joyce, T. J. Krzyzewski, G. R. Bell, B. A. Joyce, and T. S. Jones, "Composition of InAs quantum dots on GaAs(001): direct evidence for (In,Ga)As alloying," *Phys. Rev. B* **58**, R15981–R15984, 1998.
18. K. Nishi, H. Saito, S. Sugou, and J. S. Lee, "A narrow photoluminescence linewidth of 21 meV at 1.35 μm from strain-reduced InAs quantum dots covered by $In_{0.2}Ga_{0.8}As$ grown on GaAs substrates," *Appl. Phys. Lett.* **74**, 1111–1113, 1999.
19. F. Y. Chang, C. C. Wu, and H. H. Lin, "Effect of InGaAs capping layer on the properties of InAs/InGaAs quantum dots and lasers," *Appl. Physics. Lett.* **82**, 4477–4479, 2003.
20. H. Y. Liu, M. J. Steer, T. J. Badcock, D. J. Mowbray, M. S. Skolnick, F. Suarez, J. S. Ng, M. Hopkinson, and J. P. R. David, "Room-temperature 1.6 μm light emission from InAs/GaAs quantum dots with a thin GaAsSb cap layer," *J. Appl. Phys.* **99**, 046104, 2006.
21. V. A. Odnoblyudov, A. Yu. Egorov, N. V. Kryzhanovskaya, A. G. Gladyshev, V. V. Mamutin, A. F. Tsatsul'nikov, and V. M. Ustinov, "Room-temperature photoluminescence at 1.55 μm from heterostructures with InAs/InGaAsN quantum dots on GaAs substrates," *Technical Phys. Lett.* **28**, 964–966, 2002.
22. H. C. Yu, J. S. Wang, Y. K. Su, S. J. Chang, F. I. Lai, Y. H. Chang, H. C. Kuo, C. P. Sung, H. P. D. Yang, K. F. Lin, J. M. Wang, J. Y. Chi, R. S. Hsiao, and S. Mikhrin, "1.3-μm InAs–InGaAs

quantum-dot vertical-cavity surface-emitting laser with fully doped DBRs grown by MBE," *IEEE Photonics Tech. Lett.* **18**, 418–420, 2006.

23. P. S. Dutta and H. L. Bhat, "The physics and technology of gallium antimonide: an emerging optoelectronic material," *J. Appl. Phys.* **81**, 5821–5870, 1997.
24. B. R. Wu, B. F. Chu-Kung, M. Feng, and K. Y. Cheng, "High performance GaAsSb/InP double heterojunction bipolar transistors grown by gas-source molecular beam epitaxy," *J. Vac. Sci. Technol. B* **24**, 1564–1567, 2006.
25. M. W. Dvorak, C. R. Bolognesi, O. J. Pitts, and S. P. Watkins, "300 GHz InP/GaAsSb/InP double HBTs with high current capability and $BV_{CEO} > 6V$," *Electron. Device Lett.* **22**, 361–363, 2001.
26. S. C. Lee and H. H. Lin, "Transport theory of the double heterojunction bipolar transistor based on current balancing concept," *J. Appl. Phys.* **59**, 1688–1695, 1986.
27. R. Teissier, D. Sicault, J. C. Harmand, G. Ungaro, G. Le Roux, and L. Largeau, "Temperature-dependent valence band offset and band-gap energies of pseudomorphic GaAsSb on GaAs," *J. Appl. Phys.* **89**, 5473–5477, 2001.
28. S. R. Johnson, S. Chaparro, J. Wang, N. Samal, Y. Cao, Z. B. Chen, C. Navarro, J. Xu, S. Q. Yu, David J. Smith, C.-Z. Guo, P. Dowd, W. Braun, and Y.-H. Zhang, "GaAs-substrate-based long-wave active materials with type-II band alignments," *J. Vac. Sci. Technol. B* **19**, 1501–1504, 2001.
29. P.-W. Liu, G.-H. Liao, and H.-H. Lin, "1.3 μm GaAs/GaAsSb quantum well laser grown by solid source molecular beam epitaxy," *Electron. Lett.* **40**, 177–178, 2004.
30. F. Quochi, D. C. Kilper, J. E. Cunningham, M. Dinu, and J. Shah, "Continuous- wave operation of a 1.3–μm GaAsSb-GaAs quantum-well vertical-cavity surface-emitting laser at room temperature," *IEEE Photon. Tech. Lett.* **13**, 921–923, 2001.
31. G. Ungaro, et al., "GaAsSbN: a new low-bandgap material for GaAs substrates," *Electron. Lett.* **35**, 1246–1248, 1999.
32. S. Kurtz, J. Webb, L. Gedvilas, D. Friedman, J. Geisz, J. Olson, R. King, D. Joslin, and N. Karam, "Structural changes during annealing of GaInAsN," *Appl. Phys. Lett.* **78**, 748–751, 2001.
33. S. Wicaksono, S. F. Yoon, W. K. Loke, K. H. Tan, and B. K. Ng, "Effect of growth temperature on closely lattice-matched GaAsSbN intrinsic layer for GaAs-based 1.3 μm p-i-n photodetector," *J. Appl. Phys.* **99**, 104502, 2006.
34. V. Gambin, W. Ha, M. Wistey, H. Yuen, S. R. Bank, S. M. Kim, and J. S. Harris, "GaInNAsSb for 1.3–1.6μm-long wavelength lasers grown by molecular beam epitaxy," *IEEE J. Select. Topics Quantum Electron.* **8**, 795–800, 2002.
35. Z. C. Niu, S. Y. Zhang, H. Q. Ni, D. H. Wu, H. Zhao, H. L. Peng, Y. Q. Xu, S. Y. Li, Z. H. He, Z. W. Ren, Q. Han, X. H. Yang, Y. Du, and R. H. Wu, "GaAs-based room-temperature continuous-wave 1.59μm GaInNAsSb single- quantum-well laser diode grown by molecular-beam epitaxy," *Appl. Phys. Lett.* **87**, 231121, 2005.
36. Z. M. Fang, K. Y. Ma, D. H. Jaw, R. M. Cohen, and G. B. Stringfellow, "Photoluminescence of InSb, InAs, and InAsSb grown by organometallic vapor phase epitaxy," *J. Appl. Phys.* **67**, 7034–7039, 1990.
37. S. H. Wei and A. Zunger, "InAsSb/InAs: a type-I or a type-II band alignment," *Phys. Rev. B* **52**, 12039–12044, 1995.
38. S. R. Kurtz, R. M. Biefeld, A. A. Allerman, A. J. Howard, M. H. Crawford, and M. W. Pelczynski, "Pseudomorphic InAsSb multiple quantum well injection laser emitting at 3.5μm," *Appl. Phys. Lett.* **68**, 1332–1334, 1996.
39. M. E. Flatte, C. H. Grein, H. Ehrenreich, R. H. Miles, and H. Cruz, "Theoretical performance limits of 2.1–4.1 μm InAs/InGaSb, HgCdTe, and InGaAsSb lasers," *J. Appl. Phys.* **78**, 4552–4557, 1995.
40. C. Lin, M. Grau, O. Dier, and M. C. Amann, "Low threshold room-temperature continuous-wave operation of 2.24–3.04μm GaInAsSb/AlGaAsSb quantum-well lasers," *Appl. Phys. Lett.* **84**, 5088–5091, 2004.
41. R. Q. Yang, C. J. Hill, and B. H. Yang, "High-temperature and low-threshold midinfrared interband cascade lasers," *Appl. Phys. Lett.* **87**, 151109, 2005.
42. G. G. Zegrya and A. D. Andreev, "Mechanism of suppression of Auger recombination processes in type-II heterostructures," *Appl. Phys. Lett.* **67**, 2681–2683, 1995.
43. R. M. Biefeld, S. R. Kurtz, and A. A. Allerman, "Novel materials and device design by metal-organic chemical vapour deposition for use in IR emitters," *IEE Proc.-Optoelectron.* **144**, 271–276, 1997.
44. R. K. Willardson and A. C. Beer, *Semiconductors and Semimetals—Vol.* **18** *Mercury Cadmium Telluride*, Chapter 1, Academic Press, Inc., New York, 1981.
45. M. B. Reine and R. M. Broudy, A review of HgCdTe infrared detector technology, *Proc. SPIE Tech. Symp., 21*st, San Diego, CA, August 1977.
46. P. J. Lin and L. Kleinman, "Energy bands of PbTe, PbSe, and PbS," *Phys. Rev.* **142**, 478–489, 1966.
47. J. N. Zemel, J. D. Jensen, and R. B. Schoolar, "Electrical and optical properties of epitaxial films of PbS, PbTe, PbSe and SnTe," *Phys. Rev.* **140**, A330–A342, 1965.
48. T. C. Harman and I. Melngailis, *Applied Solid State Science*, Vol. **4, 1**, Academic Press, New York, 1974.
49. C. E. Hurwitz, A. R. Calawa, and R. H. Rediker, "Electron beam pumped lasers of PbS, PbSe and PbTe," *IEEE J. Quant. Electron.* **1**, 102–103, 1965.
50. U. P. Schieszl and J. Rohr, "600C lead salt laser emission near 5μm wavelength," *Infrared Phys. Technol.* **40**, 325–328, 1999.
51. Z. Feit, M. McDonald, R. J. Woods, V. Archambault, and P. Mak, "Low threshold PbEuSeTe/PbTe separate confinement buried heterostructure diode lasers," *Appl. Phys. Lett.* **68**, 738–740, 1996.

H. H. LIN
J. B. KUO
Dept. of Electrical Engineering,
National Taiwan University,
Taipei, Taiwan